



Coating Technology GmbH

## Publikationen 2005-7

### Mechanical stress in optical coatings

Georg N. Strauss

Stefan Schlichtherle

PhysTech Coating Technology GmbH  
Pflach/Austria

Hans K. Pulker

Institut für Ionenphysik, AG: Dünnschichttechnologie  
Universität Innsbruck, Innsbruck/Austria

PhysTech Coating Technology GmbH  
Kohlplatz 7, Innovationszentrum  
A-6600 Pflach  
office@phystech-coating.com  
www.phystech-coating.com

## 7. Mechanical stress in optical coatings

Georg N. Strauss

PhysTech Coating Technology GmbH, Kohlplatz 7, Innovationszentrum, A-6600 Pflach

email: office@phystech-coating.com, Internet: www.phystech-coating.com

### 1. Introduction

The mechanical properties of thin films like stress, density, adhesion, hardness, abrasion and surface structure are primarily dependent on the coating material and the kind of deposition process in use, but they are also strongly dependent on structure, microstructure, physical-chemical activity and composition. They can therefore be influenced by the production technology and the process parameters chosen. Furthermore there is a strong correlation between the mechanical properties and the optical properties of thin films.

The stress behavior of films is very important in all applications of thin films with respect to durability, stability and usability. Understanding the mechanisms that dictate the formation and evolution of film stress and developing strategies to control these stresses represent some of the most important issues in the field of thin film technology. The first investigations regarding mechanical stress in thin films were carried out in 1877 [Mills 1877] on chemically deposited films, and in a more quantitative way in 1909 [Stoney 1909]. Evaporated films were studied in the 1950's with the aim of understanding the origin of mechanical stress. Results of further measurements, explanations of the origin on stress and semi quantitative calculations of tensile stresses based on a grain boundary interaction model for crystalline films have been published in the 1979's [Hoffman et.al. 1961-1975] and [Pulker et.al. 1979]. During further investigations it was soon found that almost all films, whatever production technology is chosen, show mechanical stresses. In most thin film applications, especially in the field of optical coatings, stresses should be distinguished.

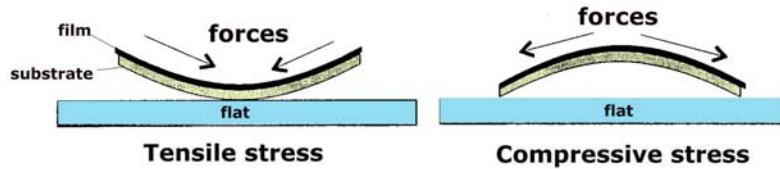


Fig. 1. Definition of compressive and tensile stress

Thin films are generally in a state of elastic mechanical stress during and after deposition. The intrinsic stress, a characteristic part of the deposition process can be tensile or compressive. Tensile stresses arise if the film tends to contract parallel to its surface and compressive stresses arise if the film expands parallel to the surface. Its sign and its magnitude are influenced by parameters such as particle energy, deposition rate, film thickness and physical and chemical incorporation of material.

The observed total mechanical stress can consist of three components according to:

$$\sigma = \sigma_{ext} + \sigma_{therm} + \sigma_{int} \quad (1)$$

The external stress ( $\sigma_{ext}$ ) arise from attack by external forces, there the thermal stress always arise if large differences exist in the thermal expansion coefficients between film material and substrate material. Strong effects can occur even during film production, at post deposition annealing or in warming up or cooling down procedures.

$$\sigma_{therm} = E_f (\alpha_f - \alpha_s) (T_p - T_m) \quad (2)$$

$E_f$  : Youngs modulus

$\alpha_f$  and  $\alpha_s$  : thermal coefficient of film and substrate

$T_p$  and  $T_m$  : temperature during evaporation process and at measurement

The last and most important part is the intrinsic stress,  $\sigma_{int}$ , in the film itself. Intrinsic stress is a structure and microstructure sensitive property which is caused by the mode of film growth and microstructural interactions, also influenced by some contaminations. Usually, the intrinsic stresses in the films are dominant, so that many investigations have dealt with them. The main mechanisms behind the origin and temporary changes of the intrinsic stresses in thin films are:

- Formation of lattice defects (microscopic voids, special arrangements of dislocations and lattice disorder)
  - Variation of the interatomic spacing (occurrence of cavities or regions of higher density in amorphous films)
  - Changes in the film structure and morphology (temporarily, dependent on process)
  - Incorporation of foreign materials or gas particles (e.g. atoms or molecules from the residual gas or working gas) and chemical reactions
  - Recrystallization processes and phase transformations during and/or after film formation
  - Differences of the lattice spacing of the substrate and the film during epitaxial film growth
- In addition, all of these processes may occur both during condensation and growth of the film and under annealing conditions afterwards. Depending on the material and the deposition conditions closed films can be vitreous or amorphous, but many are crystalline, particularly polycrystalline.

## 2. Models of the origin of intrinsic film stress

Most of the models are based on the concept that the intrinsic stress is introduced into the films due to a contraction or expansion parallel to the substrate and film surface, which leads in the first case to tensile and in the latter to compressive stresses.

A satisfactory theory for the origin of intrinsic stresses has yet to be found. The wide variation in the experimental results coupled with a still improvable knowledge of structural details has led to multiple qualitative and quantitative models. The development of stress is in most cases a combination of several effects, depending on the film material and the production process. First steps in this direction have been worked out by different groups [Heavens, Finegan 1957] and [Hoffman et.al. 1961-1975], who described the appearance of film stress by means of a combined effect of surface tension and lattice defects.

### 2.1. Defect model:

In this model the intrinsic stress is related to point defects and defect clusters, like single vacancies and interstitial migration to a free surface. In the neighborhood of such defects an elastic deformation of the lattice causes the mechanical stress [Story, Hoffman 1956], [Hoffman, Anders 1953]. The out-annealing of vacancies at temperature above 150°C leads to a stress reduction, there the total stress relief at room temperatures corresponds to a loss of about 1% vacancies. However, this point defect model is too great a simplification to account fully for the stress behavior in films and only can be applied on lower density films showing tensile stresses.

### 2.2. Surface tension model:

Surface tension can be an important contribution to the stress in thin films. Given a film with no other stress terms than the surface tension  $\gamma_1$  at the film-vacuum interface and  $\gamma_2$  at the film-substrate interface, the total apparent stress can be written as:

$$\sigma = \frac{\gamma_1 + \gamma_2}{t} \quad (3)$$

where  $t$  is the film thickness.

A positive surface energy, due to single aggregates (e.g. dimers, clusters), manifests itself as a reduced lattice constant compared with bulk material and results in a tensile film stress. An increased interatomic spacing is an indication of a negative surface energy and corresponds with compressive stress. The sign of the film stress is supposed to depend on the balance of the two effects.

### 2.3. Grain boundary model:

Most films deposited by evaporation onto unheated substrates develop a less dense, voids and gap containing, columnar microstructure which is caused by surface geometry, shadowing effects during deposition and influenced by recrystallization during deposition of thicker films. The columns consist of fairly fine prismatic crystals of the film material. This growth mode is between zone 1 and 2 of the well known MD- zone model [Movchan, Demchishin 1969]. The column boundaries are in this case like grain boundaries. The observed behavior can therefore be interpreted in terms of a stress mechanism introduced by forces at the grain boundaries of the columnar crystallites. The interaction between grain boundaries and boundary surfaces are regarded for explaining the causes, and especially the occurrence, of tensile stresses [Hoffman et.al. 1961-1975].

Frequently, pure films have tensile stresses, whose values depend on the kind of material, the deposition technique and the film thickness. Often the stresses reach a maximum when the last holes in the network film are filled. Additional thickness growth causes, along with recrystallization, a large decrease of the stresses, as can be seen in Fig.1 [Wilcock 1967], [Strauss et.al. 1997], [Floro et.al 2002].

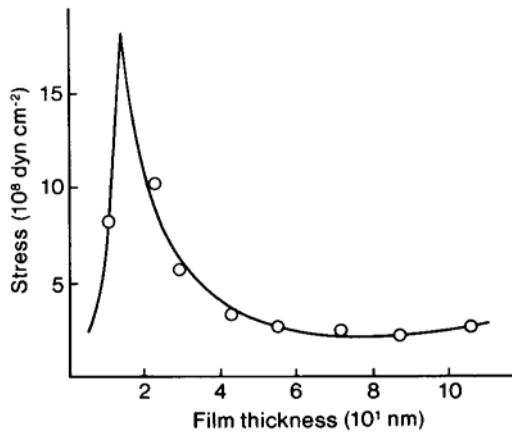


Fig. 2. General behavior of the intrinsic mechanical stress as a function of film thickness

The close approach of two free surfaces (surface energy  $\gamma_s$ ) in the formation of a grain boundary (grain boundary energy  $\gamma_{gb}$ ) results in a change in energy:

$$\Delta\gamma = 2\gamma_s - \gamma_{gb} \quad (4)$$

Part of the energy produces a constrained relaxation of the lattice atoms in the grain boundary by few percent of the unstrained lattice constant  $a$ . The elastic deformation is responsible for the macroscopically observed tensile stress according to Hook's law:

$$\sigma = Y * \varepsilon \quad \varepsilon = \frac{\Delta}{d} \quad (5)$$

where  $Y$  is Young's modulus and  $\varepsilon$  is the strain

Here  $\Delta$  is the constrained relaxation and  $d$  is the mean crystallite diameter. The average force per unit area of boundary after relaxation must equal the average elastic stress throughout the volume of the crystallite. Considering also the Poisson ratio  $\nu$  and the packing density  $p$  of the film the intrinsic stress is given by [Pulker, Mäser 1979], [Pulker 1982]:

$$\sigma = \frac{Y}{1-\nu} \frac{\Delta}{d} p \quad (6)$$

In situ measurements of the intrinsic stress in thin crystalline dielectric films have also been interpreted in terms of a stress mechanism introduced by forces at the grain boundaries of the columns [Seidel 1981].

Large grain sizes are associated with low stresses and small grain sizes with high stresses and it seems that the grain size is a dominant factor determining the magnitude of the stress. So grain growth is responsible for the observed decrease in the stress values as substrate temperature increases, thickness increases and deposition rate decreases [Sun et al. 1975].

Recently a quantitative model of the physical origin of intrinsic stress and the fundamental mechanisms that can generate stress during the growth of Volmer-Weber (V-W) thin films have been discussed [Floro et al. 2002]. In the V-W film growth, films initially grow by the nucleation of discrete islands of different crystallographic orientations, or even no crystallinity in the case of amorphous films. With ongoing deposition, the existing islands enlarge, and new islands may nucleate, until a continuous percolating network is achieved. The film continues to grow until the substrate is completely covered, followed by a additional film thickening.

During and after deposition the film undergoes several occurrences, like defect introduction, annihilation, grain growth, recrystallization or phase transitions, which cause stress within the film. This dynamic structural and microstructural evolution processes change the density of the film while the film is rigidly attached to its substrate (Doerner and Nix 1988; Nix 1989). The film will be now in a state of mechanical stress and as a consequence of the forces and moments applied to the substrate by the film, the substrate will bend slightly, which is often used to determine the resulting film stress. The evolution of the film stresses during evaporative deposition shows a so-called CTC (compressive-tensile-compressive) behaviour, which has been directly correlated with microstructural evolution (Koch 1994; Floro et al. 2001).



Fig. 2. Film growth: Nucleation – Coalescence – Continuous film (Floro et al. 2001)

The initial compressive stress occurs in the discrete-island stage of film growth, while the rapid increase in tensile stress correlates with the onset of island coalescence and grain boundary formation. The peak at the end of the tensile stress development occurs when the film becomes fully continuous, and in the final compressive stage, the continuous film is growing in thickness. CTC behaviour has been classified as a characteristic of high mobility films, whereas low mobility films exhibit only tensile stress. Surface stress is an important contribution to the stress evolution of discontinuous thin films in the discrete-island regime. Elastic deformation associated with grain boundary formation and grain growth during the coalescence process is widely regarded to be an important mechanism for tensile stress generation. The final compressive stress in continuous films can be explained by the fact that deposition occurs under highly non-equilibrium conditions in which the flux of evaporated atoms is many orders of magnitude higher than the equilibrium vapour pressure of the film at the deposition temperature. Therefore, the surface of the film is at a higher chemical potential which is the driving force for the movement of atoms into the grain boundaries and the evolution of compressive stress (Chason et al. 2001).

## 2.4. Penning model:

Thin films produced with PVD technologies without any ion or plasma assistance develop normally tensile film stress. Ion bombardment during deposition can reduce the tensile stress or even transfer tensile stress into compressive stress. The effects on the mechanical properties due to ion bombardment of the growing film are mainly depending on the kind, the amount and the energies of the involved ions, atoms and molecules. First descriptions concerning the development of compressive stress as consequence of an ion peening effect were carried out by d'Heurle (d'Heurle 1970) and later from different research groups starting in 1980 (Hoffman and Gaertner 1980; Cuomo et al. 1982; Huang et al. 1985; Windischmann 1987; d'Heurle and Harper 1989; Volkert 1991). Some calculations and computer simulations concerning the densification of the films due to ion bombardment and the effect on the microstructure of the films were carried out by Müller (Müller 1986, 1987, 1987-2). Based on such binary collision calculations a simplified but universal ion peening model explaining stress evolution and diminution due to ion bombardment was developed (d'Heurle and Harper 1989; Davis 1993; Carter 1994). According to this model compressive stress arises when the growing film is bombarded by ions, atoms or molecules with kinetic energies of tens or hundreds of

electron volt by atomic peening processes. These knock-on processes cause atoms to be incorporated into spaces in the growing film, which are smaller than the usual atomic volume.

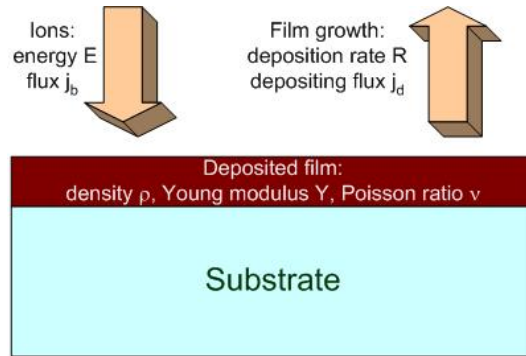


Fig. 3. Schematic diagram of a growing film with simultaneous ion bombardment of flux  $j_b$  with an energy  $E$

In order to initiate this process the impinging ions have to overcome a threshold energy  $E_{crit}$ , whose magnitude will depend on details of the film structure and composition. The compressive stress caused by implanted atoms is associated with an increase in the strain energy of the film. A reduction in the stress by movement of the implanted atoms to the film surface is energetically favoured, however, the implanted atoms are hindered from moving by repulsive forces exerted by the surrounding atoms. The implanted atoms, then, are in metastable positions within a few nanometres of the film surface. A significant fraction of the energy of a bombarding ion is transferred to violent motion, so called thermal spikes, of the atoms in the area of impact and can provide the energy required to release implanted atoms from their metastable positions within the film (Müller 1986). With these assumptions the stress can be calculated considering that there is a balance between constrained implantation and relaxation processes so that the density  $n$  of implanted atoms is constant with time. As a result of the competition between implantation and relaxation, in general the stress rises to a maximum with increasing energy of the bombarding atoms and then decreases, as can be seen in Fig.4. As a first-order approximation, the volumetric strain  $\varepsilon$  is assumed to be proportional to the fraction  $n/\rho$  of implanted atoms in the film (Windischman 1987), where  $n$  is the density of implanted atoms and  $\rho$  is the film density. For a thin film the stress is related to the strain by

$$\sigma = \frac{Y_f}{1-\nu} \varepsilon \quad (8)$$

where  $Y_f$  is the Young's modulus of the film material and  $\nu$  is the Poisson ratio. With this assumptions the stress is given by

$$\sigma \propto \frac{Y_f}{1-\nu} \frac{E^{1/2}}{j_d / j_b + k \cdot E^{5/3}} \quad (9)$$

Where  $j_d$  is the net deposition flux,  $j_b$  is the bombarding flux and  $k=0.016 \cdot C_p \cdot E_0^{-5/3}$ . This result describes the bombardment of monoenergetic ions with kinetic energies higher than  $E_{crit}$ . A range of ions may be taken into account by integrating over all energies greater than  $E_{crit}$  to give

$$\sigma = \int_{E_{crit}}^{\infty} \sigma(E) f(E) dE \quad (10)$$

where  $f(E)dE$  is the number of ions with an energy between  $E$  and  $E+dE$ .

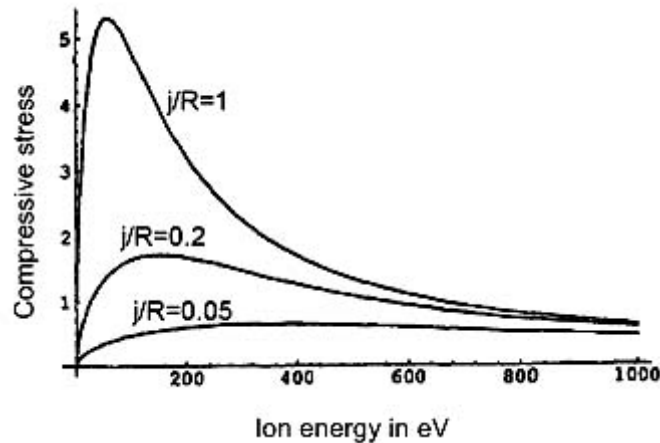


Fig. 4. Variation in compressive stress with ion energy, predicted by Eq. 9, for three values of the normalized flux  $j_b/j_d=1, 0.2$  and  $0.05$ , assuming an effective excitation energy of  $E_0=8\text{eV}$  and  $C_p=1$ , which is a material depending parameter (Davis 1993)

The model predicts that the magnitude of the compressive film stress is strongly dependent on the energy of the incident ions, with an energy dependence determined by the normalized flux  $j_b/j_d$ , where  $j_d$  is the net depositing flux and  $j_b$  is the bombarding flux. The differences in the stress-energy relationship seen in the literature can therefore be explained in terms of variations in the normalized flux. For low values of the normalized fluxes the model predicts that the film stress is proportional to the square root of the energy of the impinging ions, higher normalized fluxes, however, cause the stress to go through a maximum with increasing ion energy with a power law decrease for large energies and fluxes.

### 3. Methods of measuring stress

The determination of the intrinsic film stress is normally performed by measuring those film properties, which are changed due to the appearance of the film stress. There are several methods, which are in practical use.

The method of X-ray diffraction (XRD), and the electron diffraction method (RHEED – Reflection High Energy Electron Diffraction) determines the stress induced changes in the crystal plane distances of the lattice due to the broadening of the diffraction lines, from which the stress can be calculated. Line shifts in the diffraction diagram indicate changed lattice parameters and therefore provide information on macrostrain, whereas line broadening gives information on grain size and microstrain, i.e. lattice distortions that cause a spread around the lattice constant of the stressed material. This method is mainly used with metal films, but can also be applied for crystalline films.

Mechanical stress in solid bodies changes the inter-atomic distances and so the elastic module, which varies the velocity of sound and this can be detected by ultra sonic methods.

The piezoresistive effect consists in the change of the conductivity of a semiconductor as a consequence of an applied mechanical stress. The magnitude of the effect depends on the applied stress and its orientation with respect to the crystalline axis. The method can be applied to any pair of dielectric film-semiconductor substrate.

Several magnetic properties are connected with the atomic structure of the thin films, they can be measured to calculate the intrinsic stress.

Furthermore mechanical stress can be detected due to the change of the electrical resistance of the films or the changes in the band gap of semiconductors.

One of the well-recognized techniques to measure the stress in thin films is to determine the curvature of the bending substrate. The most general arrangements are to use a thin strip of glass clamped at one end to form a cantilever onto which the film is deposited or to use circular glass substrates or Si-wafer and determine the radius of curvature before and after deposition. The direction of the elongation of the free end indicates whether the stress is compressive or tensile.

### 3.1. Cantilever method:

In these methods bending of the substrate can be measured optically (travelling light spot), electrically (capacity change), mechanically (stylus pick up) or by electro-mechanical and magnetically means (lever in a balance measures the restoring force).

In the optical deflection measurement a one side clamped substrate strip, bearing a mirror on the rear side of its free end is used. With a projection microscope the shift of a light spot caused by bending during coating is measured with a position detector in an arrangement shown schematically in Fig.6. Careful calibration of the system is required. It is possible to detect a minimum displacement of  $10^{-4}$  cm.

It is also possible to measure the electrical capacity. In this case the cantilevered strip, silvered on its rear side, is held close and parallel to a fixed conductive plate to form part of the tuning capacity of an oscillator circuit. With the oscillator operating slightly off resonance, any change of the capacity that results from a bending of the glass strip will produce a linear change in the output of the oscillator.

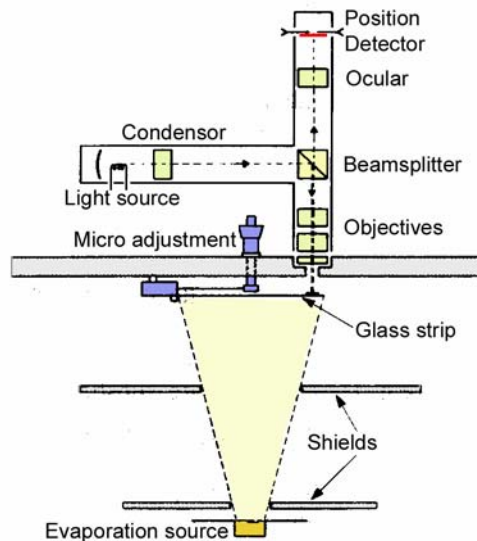


Fig. 5. Schematic diagram of an apparatus for the determination of intrinsic film stress using the cantilever method with optical detection

The electromechanical restoration method makes use of the application of a force to the free end of the strip in order to return it to the same position it was in prior to the deposition of the film. This restoring force is applied by a lever attached to the coil of an electromagnetic balance. The magnetic restoration technique is similar to the electromechanical restoration method, but in this case the restoring force is supplied by an electromagnet. This technique is limited to substrates made of, or containing some magnetic material.

### 3.2. Disk method:

The interferometric method makes use of conventional optical interference techniques to observe the bending of a thin circular glass plate. In general, this technique is limited in use in that the measurements normally must be made outside the vacuum chamber. Newton's interference rings arising in monochromatic light between an optical flat (reference) and a first uncoated and then coated glass-disc can be measured from photographic prints or a CCD. The stress induced change of the radius of curvature than can be determined and together with the elastic data of the substrate the film stress can be calculated.

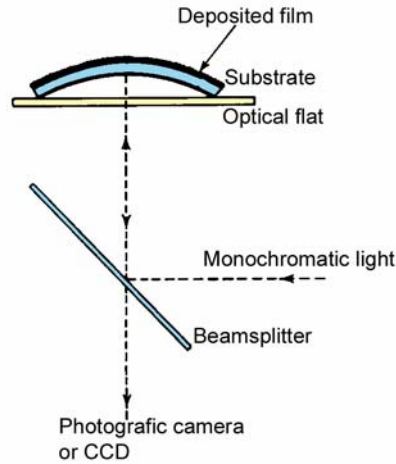


Fig. 6. Schematic representation of an apparatus for the determination of intrinsic film stress by observing Newton fringes between a stressed circular substrate and an optical flat

The change in the radius of curvature of a substrate (e.g. Si-wafer) due to progressive deposition of a stressed film is measured and the film stress value is calculated according to the following equation (Stoney 1909):

$$\sigma = \frac{Y_s t_s^2}{6(1-\nu) t_f} \frac{1}{R} \quad (11)$$

where  $\frac{Y_s}{(1-\nu)}$  (in Pa) is the biaxial elastic modulus of the substrate,  $t_s$  and  $t_f$  (in m) are the substrate and film thickness,  $R$  is the radius of curvature (in m) and  $\sigma$  is the average film stress (in Pa).

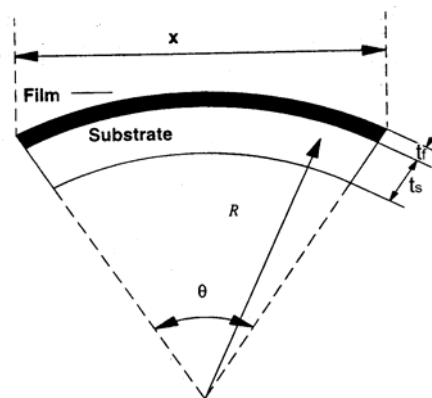


Fig. 7. Radius of curvature of a substrate due to the deposition of a film

Figure 8 shows a schematic drawing of the substrate deformed to radius  $R$  by the deposition of a film. In this case the film is under compression.

Multibeam optical stress systems are extremely sensitive and able to measure curvatures greater than  $10\text{km}$ . Since the technique is optical and the system is mounted outside the deposition chamber, it can be used for monitoring virtually any type of process as long as there is optical access to the substrate. The principle underlying this technique is also to measure the stress-induced curvature of a substrate. A single lower power laser is used where the beam is divided into a linear array of multiple parallel output beams by transmission through a etalon, which is a piece of optical glass with parallel faces, and each face has a high reflectivity optical coating. The linear beam array then reflects off the sample and is detected on a charge-coupled device (CCD) camera. The only other optics are a spatial filter, an objective lens to focus the beam on the camera and attenuating filters to prevent saturation of the CCD (Floro et al. 1996; Taylor 1997). The primary advantage is that the optics is simple and stationary, requiring only minimal alignment during initial set-up. Simultaneous detection of the entire

laser array makes the measurement inherently less sensitive to sample vibration compared with scanning mirror systems. Critical to the measurement is the use of a high resolution CCD array that enables highly accurate measurements of the spot positions. The use of image processing and data analysis routines makes it possible to detect micron-size changes in spot position.

The film stress can be calculated by a simple equation (Stoney 1909), that requires only knowledge of the film and substrate thickness, as well as the elastic modulus of the substrate:

$$\frac{1}{R} = \kappa - \kappa_0 \propto \frac{Y_f t_f \varepsilon}{Y_s t_s^2} \quad (12)$$

where  $\kappa$  is the curvature of the substrate,  $Y_f$  and  $Y_s$  are the film and substrate biaxial moduli and  $t_f$  and  $t_s$  are the film and substrate thicknesses.  $\kappa_0$  is the initial curvature of the substrate prior to film growth. It can be seen that reducing the thickness of the substrate enhances the curvature resolution. The film stress is determined directly from the curvature measurement. Determining film strain requires the biaxial modulus  $Y_f$  of the film, which is rarely known with sufficient accuracy. The challenge of this technique is to accurately detect curvature in the substrate with sufficient resolution to measure the amount of stress typically found in thin films.

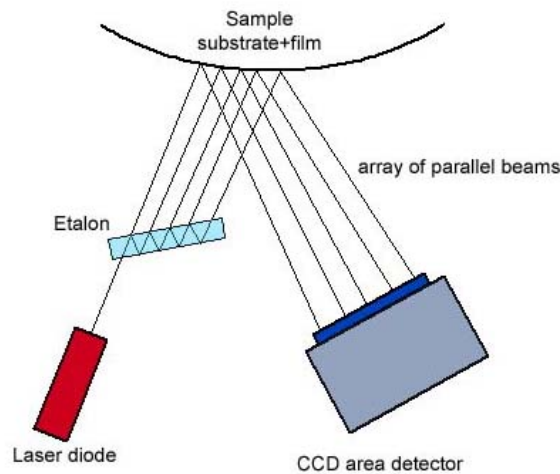


Fig. 8. Schematic diagram of a multibeam optical stress system

#### 4. Stress values in dielectric films

**Metal films:** Evaporated metal films in general show tensile stresses, whose values depend on the kind of material, the deposition technique and the film thickness.

**Metal oxide:** Metal oxide films prepared by conventional reactive evaporation (RE) have either tensile or compressive stress values, whereas those prepared by ion and plasma assisted techniques, for example ion plating (IP) and ion assisted deposition (IBAD), show nearly exclusively relatively high compressive stresses. These mostly amorphous films have a high packing density and therefore show excellent stability under changing conditions of relative humidity. The compressive intrinsic stress is a consequence of the high film density caused by higher energy of the condensing and bombarding atoms and molecules. The stress can be reduced by varying either deposition rate, gas pressure and/or the electrical parameters of the ion or plasma sources.

**SiO<sub>2</sub>:** Silicon dioxide films prepared by electron beam evaporation of fused silica show a nearly constant compressive stress of 160 MPa in 500nm thick films. Ion and plasma assistance during deposition produce a relatively large compressive stress up to 700 MPa for film thicknesses larger than 150nm. Films with thicknesses below 100nm show even higher stress values up to 1,1 GPa.

**SiO:** The stress in silicon monoxide films is very dependent on the evaporation conditions like deposition rate, gas pressure, residual gas, substrate temperature, etc. Films produced with high deposition rates (>3nm/s) at low gas pressures (<5\*10<sup>-6</sup> mbar) show relatively low stress values of 15 MPa tensile in films greater than 70nm thickness.

**MgF<sub>2</sub>:** Magnesium Fluoride develops a relatively high tensile stress, which reaches values of about 400 MPa in films with 100nm thickness. The magnitude of the stress is influenced by chemical

composition and by deposition parameters. MgF<sub>2</sub> films produced with reactive advanced plasma source ion plating (RAPSIP) show stress values from 90 MPa to 220 MPa tensile, where reactive evaporation (RE) can produce films with intrinsic stresses in the range from 30 MPa compressive to 120 MPa tensile (Atanassov et al. 1999). A permanent stress reduction in MgF<sub>2</sub> films can be achieved by the incorporation of foreign material of substances, which are insoluble in MgF<sub>2</sub> and have a low vapour pressure and low free surface energy. In this way a surface segregation of the doping material with low surface energy occurs, for example CaF<sub>2</sub> or BaF<sub>2</sub>, and produces a pronounced decrease in grain boundary interaction which results in lower stress values (Pulker 1999).

**Table 1.** Stress values of SiO<sub>2</sub> deposited with different technologies

Process	Stress in MPa	Reference
RFMS – radio frequency magnetron sputtering	-150 to -270	(Richter et al. 2001)
DCMS – direct current magnetron sputtering	-150 to -200	(Richter et al. 2001)
RAPSIP - reactive advanced plasma source ion plating	-100 to -500	(Gäbler et al. 2000)
RE - reactive evaporation	-100 to -500	(Christova and Manov 1994)
PECVD – plasma enhanced chemical vapour deposition	-70 to -80	(Ambree et al 1993) (Rutten 1989)
RIP – reactive ion plating	up to -1000	(Seddon et al 1988)
RLVIP – reactive low voltage ion plating	-500 to -1000	(Strauss et al 1997)
IBAD – ion beam assisted deposition	-10 to -470	(Robic et al 1996)
	-610 to -1900	(McNeil et al 1984)

Compressive stress: negative sign, tensile stress: positive sign

**Table 2.** Stress values of TiO<sub>2</sub> deposited with different technologies

Process	Stress in MPa	References
RAPSIP - reactive advanced plasma source ion plating	110 to 190	(Atanassov et al 1998)
RE - reactive evaporation	95	(Gäbler et al. 2000)
	165 to 300	(Atanassov et al 1998)
	220 to 300	(Szczyrbowski et al 1999) (Ottermann and Bange 1996)
MFMS – mid frequency magnetron sputtering	-500 to -900	(Szczyrbowski et al 1999)
SC – spin coating	100 to 250	(Szczyrbowski et al 1999) (Ottermann and Bange 1996)
PICVD – plasma impulse chemical vapour deposition	0 to 400	(Szczyrbowski et al 1999)
RIP – reactive ion plating	-150 to -400	(Szczyrbowski et al 1999) (Seddon et al 1988) (Ottermann and Bange 1996)
RLVIP – reactive low voltage ion plating	-800	(Pulker and Bühler 1985)
IBAD – ion beam assisted deposition	-540	(McNeil et al 1984)
FAD – filtered arc deposition	-700 to -2500	(Bendavid et al 1999)

Compressive stress: negative sign, tensile stress: positive sign

**Table 3.** Stress values of Al<sub>2</sub>O<sub>3</sub> deposited with different technologies

Process	Stress in MPa	References
RFMS – radio	-250 to -1200	(Roth et al 1987)
frequency magnetron sputtering	-200 to -300	(Qing-Shan 1989)
RE - reactive evaporation	+100	(Kubovy and Janda 1977)
RIP – reactive ion plating	-210	(Seddon et al 1988)

Compressive stress: negative sign, tensile stress: positive sign

**Table 4.** Stress values of Ta<sub>2</sub>O<sub>5</sub> deposited with different technologies

Process	Stress in MPa	References
RFMS – radio	-200 to -350	(Cheng et al 1999)
frequency magnetron sputtering		
RIP – reactive ion plating	-200	(Seddon et al 1988)
RLVIP – reactive low voltage ion plating	-400 to -1000	(Strauss et al 1997)

Compressive stress: negative sign, tensile stress: positive sign

**Table 5.** Stress values of Nb<sub>2</sub>O<sub>5</sub> deposited with different technologies

Process	Stress in MPa	References
RFMS – radio	+100 to -1100	
frequency magnetron sputtering		
DCMS – direct current magnetron sputtering	-100 to -250	(Richter et al. 2001)
RLVIP – reactive low voltage ion plating	-200 to -500	(Edlinger and Pulker 1989)

Compressive stress: negative sign, tensile stress: positive sign

## 5. Correlation between film stress and optical and mechanical film properties

Density and refractive index of isotropic materials are interrelated by the Lorentz-Lorenz equation. The mean refractive index can be calculated for the general case from

$$n_f^2 = \frac{2\overline{\rho_f}R_{mol} + M_{mol}}{M_{mol} - \overline{\rho_f}R_{mol}} \quad (13)$$

if the mean film density  $\rho_f$  is known,  $R_{mol}$  is the molar refraction, which can be calculated from single crystal data, and  $M_{mol}$  is the molar weight. If we use the packing density  $p$ , which is defined as the ratio of the average film density  $\rho_f$  and the bulk density  $\rho_m$ , the correlation between the packing density  $p$  and the refractive index  $n$  is given by:

$$p = \frac{\rho_f}{\rho_m} = \frac{n_f^2 - 1}{n_f^2 + 2} \frac{n_m^2 + 2}{n_m^2 - 1} \quad (14)$$

A linear dependence between the refractive index  $n$  and film density  $\rho_f$  can be observed for evaporated, ion- and plasma-assisted films. A strong correlation exists between the intrinsic stress and the film density. In general, evaporated films have low density, open columnar microstructure and

tensile intrinsic stress, while sputter deposited or ion plated films have higher density, close-packed microstructure and compressive stress. It is further known, that evaporated films prepared under continuous bombardment with ions of increasing kinetic energy are densified and show stress changes from tensile to compressive (Hoffman and Gaertner 1980).

One problem in highly stressed films is mechanical failures like cracking or delamination of the films. Tensile stresses cause cracks in the film perpendicular to the film plane and delamination is typical for compressive stress. Responsible for these film failures is not the film stress for itself but the elastic energy  $E_{elast}$  stored in the film. Assuming that the film stress can be considered to be biaxial and isotropic in the film plane and independent on film thickness  $t_f$ , the elastic energy  $E_{elast}$  per unit surface stored in the film is (Klockholm 1987)

$$E_{elast} = \sigma^2 \frac{(1-\nu)}{E} t_f \quad (15)$$

The mechanical stability of the film-substrate system becomes critical when the stored elastic energy approaches and exceeds a critical value  $E_{crit}$ , which is determined by a critical stress value  $\sigma_{crit}$ , and the Griffith criterion (Griffith 1920) with the crack length  $h$ , omitting  $\nu$  and surface energy  $\gamma$ .

$$E_{crit} \cong \frac{\sigma_{crit}^2 h}{E} \cong 2\gamma \Rightarrow t_{crit} \cong \frac{2E\gamma}{\sigma^2} \quad (16)$$

This demonstrates that the two new surfaces formed by a crack contribute to the total surface energy with an increase of  $2\gamma$ . When  $\sigma$  is constant and independent of film thickness  $t$  there exists a critical film thickness  $t_{crit}$  at which  $E_{elast}$  exceeds  $E_{crit}$  and film fracture will occur when  $t > t_{crit}$ . In the case of delamination the Barenblatt model (Barenblatt 1962) is more appropriate. Similar to Eq. 16 obtaining a critical energy for delamination leads to a critical stress value and finally to a critical film thickness

$$t_{crit} \cong \frac{\gamma_d E}{\sigma^2} \quad (17)$$

where the surface energy is given by  $\gamma_d = \gamma_s + \gamma_f - \gamma_i$ , (index s means substrate, f means film and i stands for the part where substrate and film were never joined).

The investigations show that, by the use of fracture theory, the criterion for film-substrate mechanical stability is dependent on  $\gamma$ ,  $\gamma_d$ ,  $\sigma$  and  $t$  and that the equations that describe the criteria for fracture and delamination have in principle the same form. To avoid catastrophic film failure,  $\sigma^2 t$  must be reduced in some manner. Varying the deposition parameters or changing the process technology can reduce the film stress.

## 6. Outlook and summary

Evaporation, sputtering and energetic ion and coating material deposition processes operated with different sets of parameters cause different structures and microstructures so that the films of the same material but produced by different technologies generally also have different stress values. Hence, the possibility exists of influencing stresses in a desired way.

In films deposited via vacuum evaporation, in the absence of any external agency (including contamination), tensile stresses are normally observed. Impurities in the deposition atmosphere of films deposited by evaporation cause the stresses to become compressive. Several mechanisms are probably involved in this phenomenon.

Theoretical treatments often explain the origin of compressive stress as a consequence of energetic particle bombardment, already discussed in chapter 2.4 Peening Model. Peening processes cause atoms to become incorporated into the growing film with a number quite higher than would be obtained otherwise since sufficient energetic atoms may be forced into spaces too small to accommodate them under thermal equilibrium conditions.

Generally, vacuum deposited films and sputter deposited films prepared at high gas pressures have tensile stresses which may be anisotropic with off-normal angle of incidence deposition. In low-pressure sputter deposition and ion plating, energetic particle bombardment gives rise to high compressive stresses due to the recoil implantations of surface atoms (Sun et al. 1975; Hoffmann and Thornton 1979; Thornton and Hoffman 1985). Studies of deposited films with concurrent bombardment have shown that the conversion of tensile to compressive stress is very dependent on the ratio of bombarding species to depositing species (Hoffman and Gaertner 1980). In plasma processing the residual film stress may be very sensitive to the substrate bias and gas pressure during deposition in a

plasma environment (Bland et al 1974; Cuthrell and Mattox 1988). The lattice strain associated with the film stress represents stored energy and this energy along with a high concentration of lattice defects leads to a lowering of the recrystallization temperature in crystalline materials, a lowered strain point in glassy materials, a high chemical etch rate, electro migration problems, void growth in metallization lines by creep or other such mass transport effects.

Film property modifications by ion bombardment are mainly caused by momentum transfer from the ions to the film atoms. Experiments on a reactive low voltage ion plating (RLVIP) process with dielectrics showed that reactive film deposition in presence of excited and ionised atoms and molecules of higher energy leads to the formation of dense chemical compound films. The high density of such films is responsible for the relatively high refractive index and the compressive stress. Ion bombardment induced local chemical defects may increase the extinction coefficient value when high ion current densities and ion energies of several tens of eV are applied in film production. Film deposition with low ion current densities and low ion energies yield stoichiometric coatings with very low extinction coefficient, low density, low stress and low refractive index. The optical and mechanical stability of such films is, however, often insufficient in such cases. The films need to be densified by a longer lasting post-deposition heat treatment at temperature higher than 300°C. This leads to a decrease in physical thickness and an increase in the refractive index and environmental stability. Heat treatment of dense films often causes microstructural relaxation phenomena and oxidation resulting in a decrease of the film density, extinction coefficient and intrinsic stress, there the physical film thickness if increased (Lechner et al 1998; Strauss et al. 1999).

As the total gas pressure of the vacuum atmosphere rises, the mean free path length in PVD processes is reduced. The paths by which neutrals, non-decelerated particles can travel or along which ionised particles can be accelerated by electrical fields are shortened. The kinetic energy of the particles impinging on the growing film decreases, which causes a decrease in growth-induced compressive stresses with rising total pressure. If the coating is deposited without applying a bias voltage, tensile stresses may even occur in the film.

If the reactive gas component of the vacuum atmosphere is increased at constant total gas pressure, the number of dissociated and ionised gas particles, which can be accelerated on to the substrate, be incorporated in the coating and contribute to the formation of the lattice, rises. As the reactive gas component increases, the propagation of reactive gas atoms in the coating will therefore also rise until certain saturation points are reached. At higher reactive gas pressures, higher compressive stresses then occur.

The coating rate of PVD processes is primarily a function of the vaporization power or sputtering power. If the particle energy is not increased, then an increase in vaporization power, and thus in the coating rate, results in a reduction in compressive stresses in PVD coatings.

As the coating thickness increases, a decrease in the growth-induced compressive stresses is generally observed. Coating failure, like delamination, may occur during or after the process where high stresses are combined with increasing coating thickness, indicating that the stresses in the interface have exceeded the limiting failure value (Pulker 1982; Hirsch and Mayr 1988; Strauss et al 1997). It will appear that a compressive stress maximum occurs in the vicinity of the interface zone, whereas stress remains virtually constant over the coating thickness in the remainder film.

The orientation of the specimens also can have an effect on the film stress. In planar sputter processes, it was noted that compressive stresses decreased if the surface of the specimen was inclined to the direction of incidence of the particles. An inclination of 45° resulted in almost complete elimination of the stresses (Hoffman 1982).

## 7. References

- Atanassov G, Turlo J, Kai Fu J, Sheng Dai Y (1999) Mechanical, optical and structural properties of TiO<sub>2</sub> and MgF<sub>2</sub> thin films deposited by plasma ion assisted deposition. *Thin Solid Films* 342, pp.83-92
- Ambree P, Kreller F, Wolf R, Wandel K (1993) Determination of the mechanical stress in plasma enhanced chemical vapour deposited SiO<sub>2</sub> and SiN layers. *J.Vac.Sci.Technol. B* 11 (3), pp.614
- Barenblatt G.I (1962) *Adv.Appl.Mech.* 7, pp.55-131
- Bendavid A, Martin P.J, Jamting A, Takikawa H, (1999) Structural and optical properties of titanium oxide thin films deposited by filtered arc deposition. *Thin Solid Films* 355-356, pp.6
- Bland R.D, Kominiak G.J, Mattox D.M (1974) Effect of ion bombardment during deposition on thick metal and ceramic deposits. *J.Vac.Sci.Technol.* 11, pp.671
- Carter G (1994) Peening in ion assisted thin films – a generalized model. *J.Phys.D:Appl.Phys.* 27, pp.1046

- Chason E, Sheldon B.W, Freund L.B, Floro J.A, Hearne S.J (2001) Phys.Rev.Lett.
- Cheng W.H, Chi S.F, Chu A.K (1999) Effect of thermal stresses on temperature dependence of refractive index for Ta<sub>2</sub>O<sub>5</sub> dielectric films. Thin Solid Films 347, pp.233-237
- Christova K.K, Manov A.H (1994) Mechanical stress and refractive index variation in dry SiO<sub>2</sub>. Int.J.Electronics 76, pp.913-916
- Cuomo J.J, Harper J.M, et.al, (1982) Modification of niobium film stress by low-energy ion bombardment during deposition. J.Vac.Sci.Technol. 20, pp. 349
- Cuthrell R.E, Mattox D.M, et.al (1988) Residual stress anisotropy, stress control, and resistivity in post cathode magnetron sputter deposited molybdenum films. J.Vac.Sci.Technol. A6(5), pp.2914
- Davis C.A (1993) A simple model for the formation of compressive stress in thin films by ion bombardment. Thin Solid Films 226, pp.30
- D'Heurle F.M. (1970) Metall.Trans. I, pp.725
- D'Heurle F.M, Harper J..M.E (1989) Note on the origin of intrinsic stresses in films deposited via evaporation and sputtering. Thin Solid Films 171, pp.81
- Doerner M.F, Nix W.D (1988) CRC Crit.Rev. Solid State Mater.Sci. 14, pp.225
- Edlinger J, Ramm J, Pulker H.K, 1989 Thin Solid Films 175, pp.207-212
- Gäbler D, Laux S, Kaiser N, Bernitzki H, (2000) Low stress and shift free optical coatings for ultra-high precision surfaces. Optical Society of America
- Griffith A.A (1920) Phil.Trans.Roy.Soc.Lond. 221, pp.163
- Floro J.A, Chason E, Lee S.R (1996) Real time measurement of epilayer strain using a simplified wafer curvature technique. Mater.Res.Soc.Symp.Proc. 406, pp.491
- Floro J.A, Hearne S.J, Hunter J.A, Kotula P, Chason E, Seel S.C, Thompson C.V (2001) J.Appl.Phys. 89, pp.4886
- Floro J.A, Chason E, Cammarata R.C, Srolovitz D.J (2002) Physical Origins of Intrinsic Stresses in Volmer-Weber Thin Films. MSR Bulletin, pp.19
- Heavens O.S, Smith S.D (1957) J.Opt.Soc.Am, 47, pp.469
- Hirsch T, Mayr P (1988) Surf.Coat.Technol. 36, pp.729-741
- Hoffman R.W, Anders F.J (1953) J.Appl.Phys, 23, pp.231
- Hoffman R.W (1975) The mechanical properties of non-metallic thin films. AEC Techn. Rep. 82, Atomic Energy Commission, Case Western Reserve University, Cleveland OH
- Hoffman D.W, Thornton J.A (1979) Effects of substrate orientation and rotation on internal stresses in sputtered metal films. J.Vac.Sci.Technol. 16(2), pp.134
- Hoffman D.W, Gaertner M.R (1980) Modification of evaporated chromium by concurrent ion bombardment. J.Vac.Sci.Technol. 17, pp.425
- Hoffman D.W (1982) Film stress diagnostics in sputter deposition of metals, Proc. 7<sup>th</sup> Int.Conf. on Vacuum Metallurgy, Tokyo
- Huang T.C, Lim G, Pramigani F, Key E (1985) Effect of ion bombardment during deposition on the x-ray microstructure of thin silver films. J.Vac.Sci.Technol. A6, pp.2333
- Klockholm E, (1987) Delamination and fracture of thin films. IBM J. Res.Develop. 31, pp.585
- Koch R, (1994) J.Phys.: Condens..Matter 6, pp.9519
- Kubovy A, Janda M (1977) Thin Solid Films 42, pp.169-173
- Lechner W, Strauss G.N, Pulker H.K (1998) Int. Conf. Coatings on Glass ICCG-98, Saarbrücken, Germany
- McNeil J.R, Barron A.C, Wilson S.R, Herrmann W.C (1984) Ion-assisted deposition of optical thin films: low energy vs. high energy bombardment. Appl.Opt. 23, pp.552-559
- Mills E.J (1877) Proc.Roy.Soc. London 26, pp.504
- Müller K.H (1986) Model for ion assisted thin film densification. J.Appl.Phys. 59, pp.2803
- Müller K.H (1987) Ion-beam induced epitaxial vapour-phase growth: a molecular dynamics study. Phys.Rev.B 35, pp.7906
- Müller K.H (1987-2) Stress and microstructure of sputter deposited thin films: molecular dynamic investigations. J.Appl.Phys. 62, pp.1796
- Movchan B.A, Demchishin A.V Study of the structure and properties of thick vacuum condensates of nickel, titanium, tungsten, aluminium oxide and zirconium dioxide. (1969) Phys.Met.Metallorg., 28, pp.83
- Nix W.D, (1989) Metall. Trans. A 20A, pp.2217
- Qing-Shan S (1989) Proc IPAT-89, Geneva, pp.64-69
- Ottermann C.R, Bange K (1996) Correlation between the density of TiO<sub>2</sub> films and their properties. Thin Solid Films 286, pp.32
- Pulker H.K, Mäser J.M (1979) The origin of mechanical stress in vacuum deposited MgF<sub>2</sub> and ZnS films. Thin Solid Films, 59, pp.65
- Pulker H.K (1982) Mechanical properties of optical films. Thin Solid Films, 89, pp.191
- Pulker H.K (1999) Coatings on Glass 2<sup>nd</sup> revd.edn., Elsevier, pp.374
- Richter F, Kupfer H, Schlott P, Gessner T, Kaufmann C (2001) Optical properties and mechanical stress in SiO<sub>2</sub>/Nb<sub>2</sub>O<sub>5</sub> multilayers. Thin Solid Films 389, pp.278-283

- Robic J.Y, Leplan H, Paulean Y, Rafin B (1996) Residual stress in silicon dioxide thin films produced by ion-assisted deposition. *Thin Solid Films* 290-291, pp.34-39
- Roth T, Kloos K.H, Broszeit E (1987) Proc IPAT-87 Brighton, UK, pp.252-257
- Rutten G.M.R (1989) Proc. IPAT-89, Geneva, pp.449-454
- Seddon R.I, Temple M.D, Klinger R.E, Tuttle-Hart T, LeFevre P.M (1988) Proc.Conf.Opt.Interference Coatings, Tucson, USA, pp.255-258
- Seidel J (1981) Stress in thin MgF<sub>2</sub> films. Thesis, University of Innsbruck, Austria
- Stoney G.C (1909) Proc.Roy.Soc. London A32, pp.172
- Story H.S, Hoffman R.W (1956) J.Appl.Phys, 27, pp.193
- Strauss G.N, Danh N.Q, Pulker H.K (1997) Mechanical stress in thin SiO<sub>2</sub> and Ta<sub>2</sub>O<sub>5</sub> films produced by reactive low voltage ion plating (RLVIP). *J.Non.Cryst.Solids*, 218, pp.256
- Strauss G.N, Lechner W, Pulker H.K (1999) Gas pressure influence on the optical and mechanical properties of Ta<sub>2</sub>O<sub>5</sub> films produced by reactive low voltage ion plating (RLVIP). *Thin Solid Films* 351, pp.53
- Sun R.C, Tisone T.C, Cruzan P.D (1975) The origin of internal stress in low-voltage sputtered tungsten films. *J. of Applied Physics*, Vol.46, No.1
- Szczyrbowski J, Bräuer G, Ruske M, Bartella J, Schroeder J, Zmely A (1999) Some properties of TiO<sub>2</sub> layers prepared by medium frequency reactive sputtering. *Surface and Coatings Technology* 112, pp.261-266
- Taylor C, Barlett D, Chason E., Floro J (1997) *Indust.Phys.*, 4 (1), pp.25
- Thornton J.A, Hoffman D.W (1985) The influence of discharge current on the intrinsic stress in Mo films deposited by cylindrical and planar magnetron sputtering sources. *J.Vac.Sci.Technol.* A3, pp.576
- Volkert C.A (1991) Stress and plastic flow in silicon during amorphization by ion bombardment. *J.Appl.Phys.* 70, pp.3521
- Wilcock J.D (1967) Stress in thin films, Thesis, Imperial College, University of London
- Windischmann H (1987) An intrinsic stress scaling law for polycrystalline films prepared by ion beam sputtering. *J.Appl.Phys.* 62, pp.1800

## 8. List of symbols and abbreviations

$\sigma$	mechanical stress	$\sigma, \sigma_{\text{ext}}, \sigma_{\text{therm}}, \sigma_{\text{int}}$
Y	Young's modulus	$Y_f, Y_s$
$\alpha$	thermal coefficient	$\alpha_f, \alpha_s$
T	temperature	
$\tau$	surface tension	
t	thickness	$t_f, t_s$
$\gamma$	surface energy: $\gamma_s, \gamma_{\text{gb}}, \gamma_d, \gamma_f, \gamma_i$	
$\varepsilon$	strain	
a	lattice constant	
$\Delta$	constrained relaxation	
d	diameter	
$\nu$	Poisson ratio	
p	packing density	
E	energy	$E, E_{\text{elast}}, E_{\text{crit}}$
j	flux	$j_{\text{bomb}}, j_{\text{depos}}$
$\rho$	density	$\rho_f$
n	particle density	
n	refractive index	
C	constants	$C_p$
R	radius	
$\kappa$	curvature	